International Journal of Fracture (2006) 138:211–218
DOI 10.1007/s10704-006-0030-6 © Springer 2006

Laboratory earthquakes

ARES J. ROSAKIS[1,*], HIROO KANAMORI[2] and KAIWEN XIA[3]
[1]*Graduate Aeronautical Laboratories, California Institute of Technology, Pasadena, CA 91125, USA*
[2]*Seismological Laboratory, California Institute of Technology, Pasadena, CA 91125, USA*
[3]*Department of Civil Engineering, University of Toronto, 35 St. George Street, Toronto, ON M5S 1A4, Canada*
[*]*Author for correspondence (E-mail: rosakis@aero.caltech.edu)*

Received 1 March 2005; accepted 1 December 2005

Abstract. We report on the experimental observation of the phenomenon of, spontaneously nucleated, supershear rupture and on the visualization of the mechanism of subRayleigh to supershear rupture transition in frictionally-held interfaces. The laboratory experiments mimic natural earthquakes. The results suggest that under certain conditions supershear rupture propagation can be facilitated during large earthquakes.

Key words: Earthquake rupture, supershear, subRayleigh, transition.

1. Introduction

Vertically dipping crustal faults are long pre-existing weak planes that extend tens of kilometers perpendicularly to the earth's surface and often host catastrophic earthquake rupture events. The geometry (planarity and length) of such faults is often simple enough to apply appropriately modified concepts of dynamic fracture mechanics to the study of the physics underlying their rupture process. Due to the nature of earthquakes however, direct full field and real time observations of the rupture process are prohibited while even strong motion data have limitations of spatial resolution. As a result, most efforts to date have focused on complicated analytical studies and on extensive numerical modeling of dynamic rupture processes using finite element, finite difference, and boundary element methods. As clearly elucidated by Rice et al. (2001), the nature and stability of the predicted rupture process depends very strongly on the choice of cohesive or frictional laws employed in the modeling and, as a result, experimental validation of the fidelity of such calculations becomes of primary importance.

Despite continuous efforts starting from the early 1970's (Dieterich, 1972; Brune, 1973; Dieterich and Kilgore, 1994; Anooshehpoor and Brune, 1999), there are still many mysteries regarding earthquake rupture dynamics. One of the pressing questions relevant to Seismic hazard is how fast real earthquake ruptures can propagate. As shown by Rosakis (Rosakis et al., 1999), shear cracks in coherent, adhesive, engineering interfaces can propagate at a supershear velocity (faster than the shear wave speed of the material) in various bonded bimaterials subjected to impact loading. However, questions remain about the possibility of supershear growth of a frictional, earthquake type, ruptures whose nucleation is spontaneous in nature (absence

of stress wave loading) and whose propagation takes place on a mostly frictional, incoherent, interface. In this paper we describe work in progress related to the scientific questions posed above. This work capitalizes heavily on scientific knowledge on shear fracture processes in heterogeneous, engineering material systems and layered structures of the type studied in the past 10 years at Caltech under our engineering composites program. The scientific principles obtained through our past work have been extended to the study of a dynamic rupture problem that occurs over length scales that are 5–6 orders or magnitude larger than the equivalent engineering applications.

2. Recent reports of supershear earthquake fault rupture

The M_s 8.1 (M_w 7.8) central Kunlunshan earthquake that occurred on 14 November, 2001, was an extraordinary event from the point of view of dynamic rupture mechanics. The rupture occurred over a long, near-vertical, strike-slip fault segment of the active Kunlunshan fault and featured an exceptionally long (400 km) surface rupture zone and large surface slip displacements (Lin et al., 2002). Modeling of the rupture speed history (Bouchon and Vallee, 2003) suggests rupture speeds that are slower than the Rayleigh wave speed, c_R, for the first 100 km, transitioning to supershear for the remaining 300 km of rupture growth. Other events, such as the 1979 Imperial Valley earthquake (Archuleta, 1984; Spudich and Cranswick, 1984), the 1992 Landers earthquake (Olsen et al., 1997), the 1999 Izmit earthquake (Bouchon et al., 2001), and the 2002 Denali earthquake (Ellsworth et al., 2004) may also have featured supershear speeds. Supershear was also predicted theoretically (Burridge, 1973; Burridge et al., 1979) and numerically (Andrews, 1976; Das and Aki, 1977). Even with these estimates and predictions at hand, the question of whether natural earthquake ruptures can propagate at supershear speeds is still a subject of active debate. In addition, the exact mechanism for transition from subRayleigh (speed earthquake-type rupture starts with) to supershear rupture speed is not clear. One answer to this question was provided by the 2-D Burridge–Andrews Mechanism (BAM) (Andrews, 1976) which is a mechanism introduced to circumvent restrictions imposed by classical fracture mechanics theories. Classical dynamic fracture theories of growing shear cracks have many similarities to the earthquake rupture processes. Such theories treat the rupture front as a distinct point (sharp tip crack) of stress singularity. Such conditions are closer to reality in cases that feature coherent interfaces of finite intrinsic strength and toughness. The singular approach ultimately predicts that dynamic shear fracture cannot propagate in the small velocity interval between C_R and C_S, the shear wave speed of the material, and thus excludes the possibility of a smooth transition from subRayleigh to supershear. The introduction of a distributed rupture process zone has allowed fracture mechanics to better approximate the conditions that exist during real earthquake events (Rosakis, 2002) and to describe mechanisms for a subRayleigh rupture to enter the supershear regime. According to the two-dimensional BAM, a shear rupture accelerates to a speed very close to c_R soon after its initiation. A peak in shear stress is found to propagate at the shear wave front and is observed to increase its magnitude as the main rupture speed approaches c_R. At that point, the shear stress peak may become strong enough to promote the nucleation of a secondary micro-rupture whose leading edge propagates at c_P, the P wave speed of

the material. Shortly thereafter, the two ruptures join up and the combination propagates at c_P (Rosakis, 2002). Recent numerical investigations of frictional rupture have suggested alternative, asperity based, three dimensional mechanisms (Day, 1982; Madariaga and Olsen, 2000; Dunham et al., 2003). Whether and how supershear rupture occurs during earthquakes has important implications for seismic hazards because the rupture speed influences the character of near-field ground motions.

3. The experiments

To answer the above stated questions, we conducted experiments that mimic the earthquake rupture processes. Our goal was to examine the physical plausibility and conditions under which supershear ruptures can be generated in a controlled laboratory environment. We studied spontaneously nucleated dynamic rupture events in incoherent, frictional interfaces held together by far-field tectonic loads. Thus we departed from experimental work that addresses the dynamic shear fracture of coherent interfaces loaded by stress waves (Rosakis et al., 1999; Rosakis, 2002) which was of direct relevance to the dynamic failure of Naval structures. In this study, a fault is simulated using two photoelastic plates (Homalite) held together by friction and the far-field tectonic loading is simulated by far-field pre-compression (Figure 1a–c). A unique device that triggers the rupture in a highly controlled manner is used to nucleate the dynamic rupture while preserving the spontaneous nature of the rupturing. This triggering is achieved by an exploding wire technique. The fault forms an acute angle with the compression axis to provide the shear driving force for continued rupturing.

The triggering mechanism is inspired by recent numerical work on rupture along frictional interfaces (Rice et al., 2001). Experimentally, it is a convenient way of triggering the system's full-field, high-speed diagnostics (Figure 1a) that would otherwise be unable to capture an event with total duration of $\sim 50\mu$s.

More than 50 experiments featuring a range of α and far-field pressure P were performed and the symmetric bilateral rupture process histories were visualized in intervals of 2μs. Depending on P and α, rupture speeds that are either subRayleigh or supershear were observed. The maximum shear stress field for an experiment with $\alpha = 25^\circ$ and $P = 7$ MPa (Figure 2a) shows that the speed of the rupture tip is very close to c_R and follows closely behind the circular shear wave front which is emitted at the time of rupture nucleation. The same was found to be true for smaller angles and lower pressures. For an experiment with $\alpha = 25^\circ$ and $P = 15$ MPa (Figure 2b), the circular trace of the shear wave is also visible and is at the same location as in Figure 2a. However, in front of this circle a supershear disturbance, featuring a Mach cone (pair of shear shock waves) is clearly visible. For this case, the sequences of images before 28μs have a similar form to the image displayed in Figure 2b, and reveal a disturbance that was nucleated as supershear. Its speed history $v(t)$ is determined independently by either the rupture length record or by measuring the inclination angle, β, of the shear shocks with respect to the fault plane and using the relation $v = c_S/\sin\beta$. Its speed was 1970 m/s, which is close to the longitudinal wave speed c_P. In previous experiments involving strong, coherent, interfaces and stress wave loading, stable rupture speeds near $\sqrt{2}c_S$ were observed (Rosakis et al., 1999). This apparent discrepancy can be explained by referring to the rupture

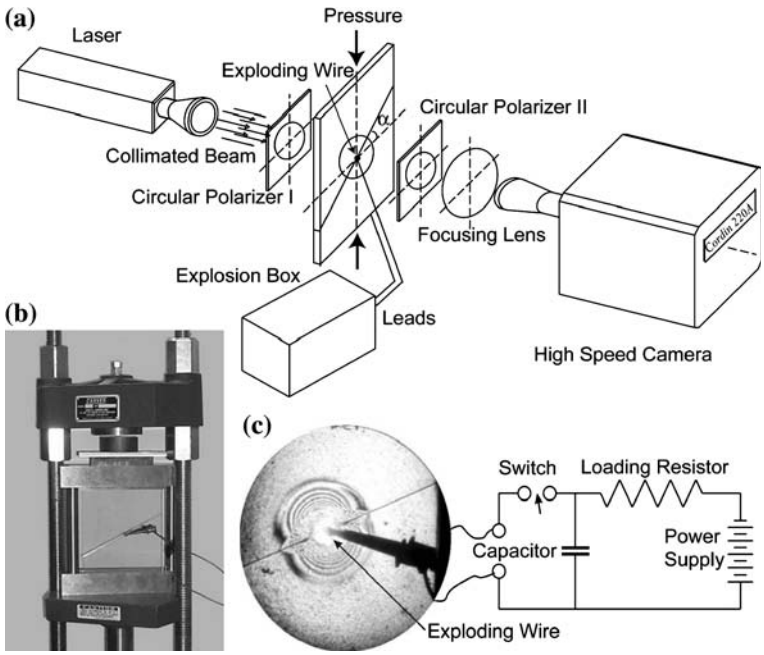

Figure 1. The diagnostics is photoelasticity combined with high-speed photography (up to 10^8 frames/s). The fault system is simulated by using two photoelastic plates (Homalite-100, shear modulus G = 1.4 GPa, Poisson's ration $\nu = 0.35$, density $\rho = 1200\,\mathrm{kg/m^3}$) held together by friction. The interface (fault) is inclined at an angle α to the horizontal promoting strike-slip rupture events (a). The carefully prepared interface has a measured static coefficient of friction $\mu^s = 0.6$; the dynamic coefficient of friction μ^d is estimated by finding the critical α of triggered events, which is between 10° and 15°, and hence $\mu^d = 0.2$ is estimated. The far-field tectonic loading is simulated by uniaxial compression exerted at the top and bottom ends of the system by a hydraulic press (b). The dynamic rupture is nucleated at the center of the simulated fault by producing a local pressure pulse in a small area of the interface. A thin wire of 0.1 mm in diameter is inserted in a small hole of the same size. An electronic condenser is then discharged turning the metal into expanding plasma to provide the controllable pressure pulse (c).

velocity dependence on the available energy per unit crack advance within the supershear regime (Rosakis, 2002). This energy attains a maximum value at speeds closer to $\sqrt{2}\,c_S$ for strong interfaces while for weaker interfaces, this maximum moves towards c_P.

To visualize a transition within our field of view (100 mm), we kept $\alpha = 25^\circ$ but reduced P to 9 MPa (Figure 3a–c). The circular traces of P and S waves are visible followed by a rupture propagating initially at c_R (Figure 3a). A small secondary rupture appears in front of the main rupture and propagates slightly ahead of the S wave front (Figure 3b). The two ruptures coalesce and the leading edge of the resulting rupture grows at a speed close to c_P. The transition length L here is ~ 20 mm (Figure 3d).

4. Modeling and conclusions

The above transition phenomenon is comparable with BAM, which was described by Andrews (1976). Andrews investigated this transition in a parameter space spanned

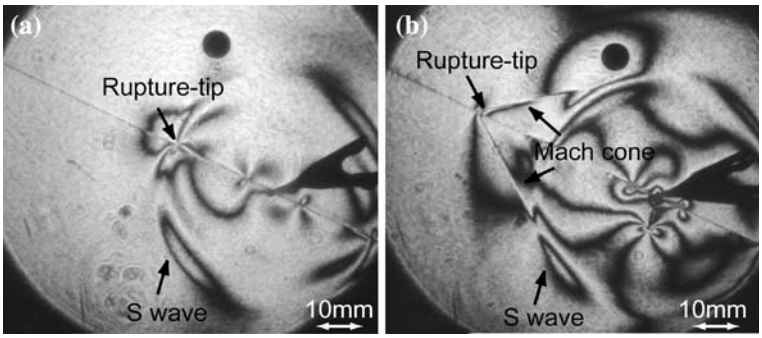

Figure 2. Purely subRayleigh ($\alpha = 25^\circ$, $P = 7$ MPa) (a) and purely supershear ($\alpha = 25^\circ$, P = 15 MPa) (b) rupture at the same time (28μs) after triggering.

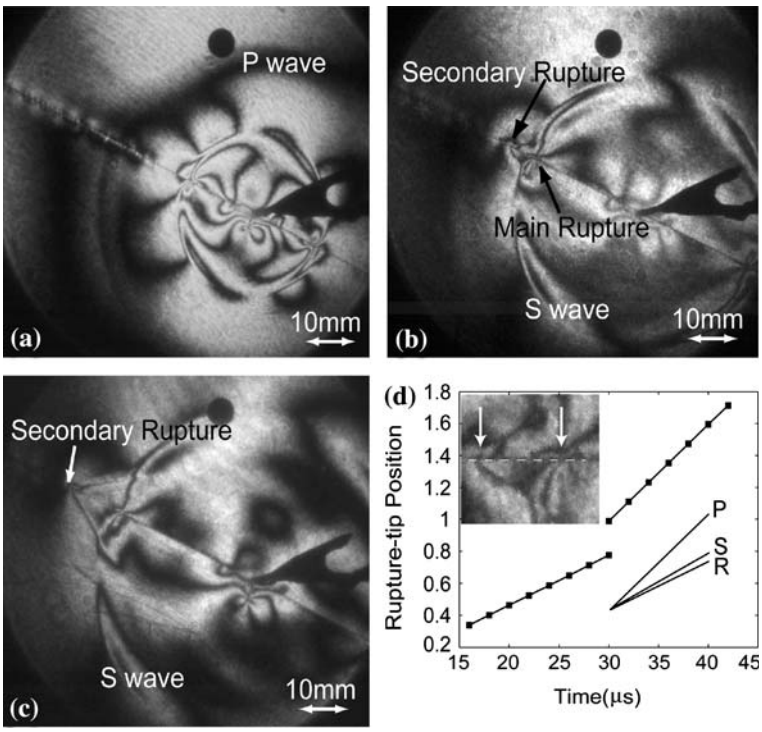

Figure 3. Visualization of the subRayleigh to supershear rupture transition ($\alpha = 25^\circ$ $P = 9$ MPa). (a–c) were taken at 18μs, 30μs and 38μs respectively. In the rupture-tip history plot (d), we included lines corresponding to P, S and Rayleigh waves as reference.

by a normalized supershear transition length L/L_c and a non-dimensional driving stress parameter s ($s = (\tau^y - \tau)/(\tau - \tau^f)$). The parameters τ, τ^y and τ^f are the resolved shear stress on the fault, the static and the dynamic strength of the fault, respectively, which describe the linear slip-weakening frictional law. In our experiment, s, can be expressed as $s = (\mu^s \cos\alpha - \sin\alpha)/(\sin\alpha - \mu^d \cos\alpha)$. Andrews' result can be written as $L = L_c f(s)$, where the function $f(s)$ has been given numerically and can be approximated by $f(s) = 9.8(1.77 - s)^{-3}$. The normalizing length L_c is the critical length for unstable rupture nucleation and is proportional to the rigidity G and

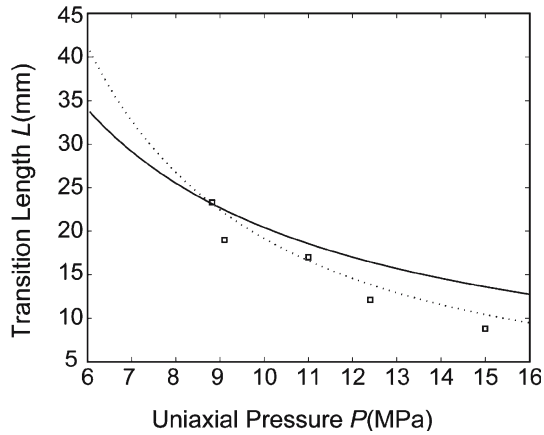

Figure 4. Transition length as a function of far-field load. Solid curve is Andrew's theory, dashed curve is modified theory and squares are experimental data.

to d_0, which is the critical or breakdown slip of the slip weakening model. L can then be expressed as:

$$L = f(s)[(1+\nu)/\pi][(\tau^y - \tau^f)/(\tau - \tau^f)^2]Gd_0. \tag{1}$$

Applying Equation 1 to our experiments, the transition length is inversely proportional to the applied uniaxial pressure P as:

$$L = f(s)\,[(1+\nu)/\pi]\,G\left[(\mu^s - \mu^d)/(\tan\alpha - \mu^d)^2\right](d_0/P)\,. \tag{2}$$

We can compare our experiments to Andrews' theory (Figure 4). Although the theory qualitatively captures the trends of the experiments, the data exhibits a dependence on pressure stronger than P^{-1}.

A natural way to modify Andrews' results is to introduce some micro-contact physics, and to thus consider the effect of pressure on d_0. We first note that there exists a linear relation between a characteristic surface length (half-distance between contacting asperities, D) and the critical slip distance $d_0(d_0 = c[(\tau^y - \tau^f)/\tau^f]^M D$, where c and M are constants) (Xia et al., 2004). We then denote the normal stress applied on the fault as $\sigma(\sigma = P\cos^2\alpha)$ and assume that the average radius of n contacting asperities, a_0, is constant. As the pressure over a macroscopic contact area $A(=n\pi D^2)$ is increased, n, as well as the real contact area $A_r(=n\pi a_0^2)$ increase. By defining the hardness H as the ratio of the normal force N to A_r, N can be expressed as: $N = HA_r = \sigma A = AP\cos^2\alpha$. Substitution of A and A_r in terms of D and a_0 respectively, gives $D = \sqrt{H}a_0\cos\alpha P^{-1/2}$. Using the relation $d_0 \propto D$, d_0 is found to depend on the pressure as $d_0 \propto P^{-1/2}$. By further using Equation 2, a modified expression relating L to P emerges featuring a stronger pressure dependence ($L \propto P^{-3/2}$). This modified relation which agrees well with the experimental data (Figure 4) is given by:

$$L = f(s)\frac{1+\nu}{\pi}G\frac{\mu^s - \mu^d}{[\sin\alpha - \mu^d\cos\alpha]^2}2c\left(\frac{\mu^s - \mu^d}{\mu^s}\right)^M \sqrt{H}a_0P^{-\frac{3}{2}}\cos^{-1}\alpha. \tag{3}$$

For seismic applications, we rewrite Equation 1 in terms of the effective stress $\tau_e = \tau - \tau^f$ as $L = f(s)(1+\nu)(1+s)Gd_0/\pi\tau_e$. Application of this equation to both seismic

faulting and to laboratory data allows us to scale L from laboratory to seismological conditions. The stress τ_e in our experiments is chosen to be of the same order as that in seismology. The ratio of rigidity of the Earth's crust to Homalite is 25. We estimate $L = 20$ mm from the experiment where $P = 9$ MPa and $\alpha = 25°$, and for which $d_0 = 10\mu$m (obtained using Equation 2). The values of d_0 for large earthquakes are often estimated as 50 cm to 1 m (Xia et al., 2004). Thus, if s is approximately the same under laboratory and crustal conditions, L for earthquakes can be estimated to be in the range between 25 and 50 km. Because s can be different, and the estimate of d_0 for earthquakes is uncertain, this value should be taken as an order of magnitude estimate. Nevertheless, it is of the same order as that inferred for the Kunlunshan event (Bouchon and Vallee, 2003).

The large L required for supershear is one of the reasons why only a few earthquake events have been observed to feature supershear speeds. It suggests that in such cases the tectonic stress is fairly close to the static fault strength (i.e., small s), which has important implications for evolution of rupture in large earthquakes.

Acknowledgements

Authors appreciate fruitful discussions with T. Heaton and G. Ravichandran from Caltech and J. R. Rice from Harvard. This study is supported by NSF grant EAR-0207873 and Naval Research grant N00014-03-1-0435 (Yapa D. S. Rajapakse program monitor).

References

Andrews, D.J. (1976). Rupture velocity of plane strain shear cracks. *Journal of Geophysical Research* **81**(32), 5679–5687.

Anooshehpoor, A. and Brune, J.N. (1999). Wrinkle-like weertman pulse at the interface between two blocks of foam rubber with different velocities. *Geophysical Research Letters* **26**(13), 2025–2028.

Archuleta, R.J. (1984). A faulting model for the 1979 imperial-valley earthquake. *Journal of Geophysical Research* **89**(NB6), 4559–4585.

Bouchon, M., Bouin, M.P., Karabulut, H., Toksöz, M.N., Dietrich, M. and Rosakis, A.J. (2001). How fast is rupture during an earthquake? New insights from the 1999 Turkey earthquakes. *Geophysical Research Letters* **28**(14), 2723–2726.

Bouchon, M. and Vallee, M. (2003). Observation of long supershear rupture during the magnitude 8.1 Kunlunshan earthquake. *Science* **301**(5634), 824–826.

Brune, J.N. (1973). Earthquake Modeling by stick-slip along precut surfaces in stressed form rubber. *Bulletin of the Seismological Society of America* **63**(6), 2105–2119.

Burridge, R. (1973). Admissible speeds for plane-strain self-similar shear cracks with friction but lacking cohesion. *Geophysical Journal of the Royal Astronomical Society* **35**(4), 439–455.

Burridge, R., Conn, G. and Freund, L.B. (1979). Stability of a rapid mode-ii shear crack with finite cohesive traction. *Journal of Geophysical Research* **84**(NB5), 2210–2222.

Das, S. and Aki, K. (1977). Numerical study of 2-dimensional spontaneous rupture propagation. *Geophysical Journal of the Royal Astronomical Society* **50**(3), 643–668.

Day, S.M. (1982). 3-Dimensional simulation of spontaneous rupture – the effect of nonuniform prestress. *Bulletin of the Seismological Society of America* **72**(6), 1881–1902.

Dieterich, J.H. (1972). Time-dependent friction as a possible mechanism for aftershocks. *Journal of Geophysical Research* **77**(20), 3771–3781.

Dieterich, J.H. and Kilgore, B.D. (1994). Direct observation of frictional contacts – new insights for state-dependent properties. *Pure and Applied Geophysics* **143**(1–3), 283–302.

Dunham, E.M., Favreau, P. and Carlson, J.M. (2003). A supershear transition mechanism for cracks. *Science* **299**(5612), 1557–1559.

Ellsworth, W.L., Çelebi, M., Evans, J.R., Jensen, E.G., Nyman, D.J. and Spudich, P. (2004). Processing and Modeling of the Pump Station 10 Record from the November 3, 2002, Denali Fault, Alaska Earthquake. Eleventh International Conference of Soil Dynamics and Earthquake Engineering, Berkeley, California, January 7–9.

Lin, A.M., Fu, B.H., Guo, J.M., Zeng, Q.L., Dang, G.M., He, W.G. and Zhao, Y. (2002). Co-seismic strike-stip and rupture length produced by the 2001 M-s 8.1 Central Kunlun earthquake. *Science* **296**(5575), 2015–2017.

Madariaga, R. and Olsen, K.B. (2000). Criticality of rupture dynamics in 3-D. *Pure and Applied Geophysics* **157**(11–12), 1981–2001.

Olsen, K.B., Madariaga, R. and Archuleta, R.J. (1997). Three-dimensional dynamic simulation of the 1992 Landers earthquake. *Science* **278**(5339), 834–838.

Rice, J.R., Lapusta, N. and Ranjith, K. (2001). Rate and state dependent friction and the stability of sliding between elastically deformable solids. *Journal of the Mechanics and Physics of Solids* **49**(9), 1865–1898.

Rosakis, A.J. (2002). Intersonic shear cracks and fault ruptures. *Advances in Physics* **51**(4), 1189–1257.

Rosakis, A.J., Samudrala, O. and Coker, D. (1999). Cracks faster than the shear wave speed. *Science* **284**(5418), 1337–1340.

Spudich, P. and Cranswick, E. (1984). Direct observation of rupture propagation during the 1979 imperial valley earthquake using a short baseline accelerometer array. *Bulletin of the Seismological Society of America* **74**(6), 2083–2114.

Xia, K.W., Rosakis, A.J. and Kanamori, H. (2004). Laboratory earthquakes: the sub-rayleigh-to-supershear rupture transition. *Science* **303**, 1859–1861.